3.4 COMPARISON OF THE LEVEL OF NEUTRAL BUOYANCY OBSERVED FROM SOUNDINGS AND RADAR

Amanda J. Homann*, Gretchen L. Mullendore, Jeffrey S. Tilley, and Scott T. Jorgenson
University of North Dakota, Grand Forks, ND

1. INTRODUCTION

Rapid vertical transport of heat, moisture, and chemical tracers from the boundary layer to the upper troposphere and lower stratosphere is accomplished primarily through moist convection (e.g. Dickerson 1987). Simulations of convective mass transport have been done (e.g. Stenchikov et al. 1996; Mullendore et al. 2005), but with limited observational networks, these results are relatively unconstrained. In order for atmospheric chemistry models to correctly simulate the upper troposphere and lower stratosphere, the level at which mass is being detrained must be correctly simulated.

In addition, recent studies (e.g. Schumacher et al. 2004; Alexander et al. 2004) have shown that updraft size and extent relate closely to heating profiles and water vapor transport which play a significant role in the global momentum and radiative budgets. Earlier work illustrates that the vertical structure of hydrometeors and kinematic quantities such as horizontal divergence, vertical air motion, and vertical mass flux all supply important information to the location of latent heat release (Tao et al. 1993; Mapes and Houze 1995; Kummerow et al. 1996; Olson et al. 1999; Yang and Smith 1999).

The level of neutral buoyancy (LNB) or the height at which parcel theory estimates that the updraft begins slowing down, is most simply estimated by lifting a representative parcel of air from the surface to the level at which air is no longer positively buoyant. Modeling work done by Raymond and Blyth (1986) shows that parcels aggregate at their LNB indicating detrainment is maximized at this level.

The LNB is generally estimated from radiosonde data; however, using the LNB determined from environmental soundings as a proxy for the detrainment height may be unrepresentative in many convective situations. One reason for this is the high spatial and temporal variability between sounding stations which is normally unobserved except in extensive field experiments. This variability results in different parcel properties and estimated detrainment heights. Also, the LNB is likely varying in time as the storm continues to mature and dissipate. There are many situations in which convection forms and propagates across an area where environmental soundings are not available at that specific time or location and an estimation of the LNB is simply unknown.

*Corresponding author address: Amanda J. Homann, Univ. of North Dakota, Dept. of Atmospheric Sciences, Grand Forks, ND 58202-9006; e-mail: amanda.homann@und.edu

A second reason why the LNB determined from environmental soundings is unrepresentative is the use of parcel theory, which introduces several assumptions that may or may not be representative of actual updraft trajectories. Parcel theory neglects the vertical perturbation pressure gradients producing an inaccurate picture of parcel accelerations (Doswell and Markowski 2004) and therefore inaccurate detrainment height estimates. One such assumption is that there is no entrainment of environmental air into the updraft which would more than likely reduce buoyancy and detrainment heights. Entrainment amounts and profiles can be approximated (e.g. Emanuel 1991; Kain and Fritsch 1990), but entrainment itself is also highly variable, depending on factors such as the local environmental profile (CAPE and CIN), storm classification, and storm size (Cohen 2000; Mullendore et al. 2005).

Another assumption is that the most representative convective updraft parcel is one that begins at the surface. Values estimated using parcel theory are wholly dependent on the choice of the base state (Doswell and Markowski 2004). Therefore, using parcel theory to find the LNB may not always be the most accurate method to finding storm deposition heights. In order for cloud-resolving transport models to correctly simulate convective situations, a direct measurement of the height at which storm outflow actually occurred is then needed.

2. DATA

Dual-Doppler radar data (vertical velocity and divergence fields) from several field campaigns were utilized to calculate observed detrainment heights for several case studies. Environmental soundings obtained during each campaign were used to understand the convective environment before and during each storm.

2.1 *TRMM-LBA*

The first storm studied was observed during the Tropical Rainfall Measuring Mission Large-Scale Biosphere-Atmosphere (TRMM-LBA) field campaign conducted in Rondonia, Brazil. The observational platforms for TRMM-LBA included four radiosonde sites and two radars, the NASA TOGA C-band radar and the NCAR S-band radar (S-pol). Specifications for each of the radars can be found in Table 1 of Lang and Rutledge (2002). Sounding and radar locations for the TRMM-LBA campaign can be seen in Fig. 1. This study incorporates all of the sounding data available for 26 January 1999 at the Abracos Hill, Rebio Jaru, and Rolim de Moura sites. No data were collected on this date at the Rancho Grande site.

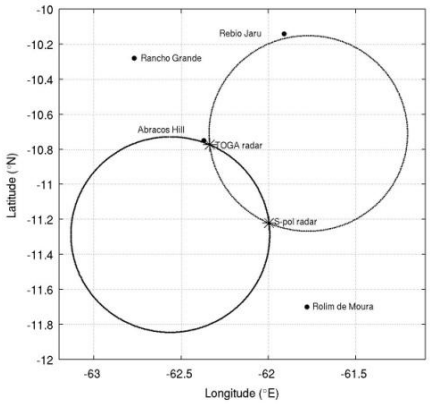

Fig. 1. Sounding and radar locations for the TRMM-LBA campaign. Circles represent dual-Doppler lobes with a crossing angle of 30°.

As stated in Cifelli et al. (2002), the unfolded radial velocity data were interpolated onto a 1.0 km horizontal resolution and a 0.5 km vertical resolution Cartesian grid centered on the S-pol radar using the NCAR REORDER software package (Mohr et al. 1986). Dual-Doppler analyses were then performed using the NCAR Custom Editing and Display of Reduced Information in Cartesian Space (CEDRIC) software package (Mohr and Miller 1983). A variational integration technique was used in the dual-Doppler processing of the vertical velocity field. A complete explanation of the radar quality control issues can be found in Cifelli et al. (2002).

The first storm studied was a squall line that went through the TRMM-LBA dual-Doppler domain on 26 January 1999. The squall line formed at an outflow boundary from previous convection several hundred kilometers northeast of the TRMM-LBA sampling domain (Cifelli et al. 2002). The MCS entered the eastern dual-Doppler lobe around 1950 UTC (Fig. 2) as a strong convective line oriented roughly north-south. Radar CAPPIs of reflectivity indicate the MCS was beginning to transition from the intensifying to mature stage around 2000 UTC. The system continued to move westward across the dual-Doppler domain before merging with an east-west oriented convective complex that had formed ahead of the line around 2100 UTC.

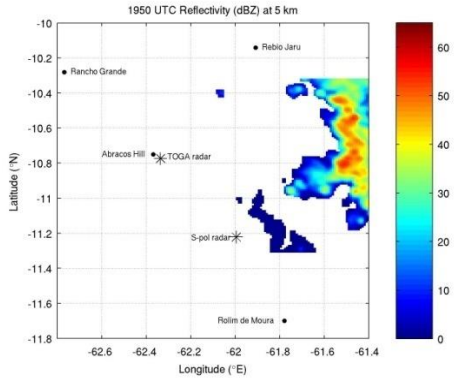

Fig. 2. Horizontal cross section of the LBA squall line at a height of 5 km (1950 UTC).

2.2 *STEPS*

The Severe Thunderstorm Electrification and Precipitation Study (STEPS) field campaign took place in the central United States. Radars operated during the STEPS field campaign included the CSU-CHILL radar and the NCAR S-pol polarimetric radars. Specifications for each of these radars can also be found in Table 1 of Lang and Rutledge (2002). The STEPS campaign also incorporated three NWS sounding locations and numerous mobile soundings. This study incorporates all of the mobile soundings available for this date while future work will incorporate data from the NWS soundings. Fig. 3 displays the sounding and radar locations for the STEPS campaign.

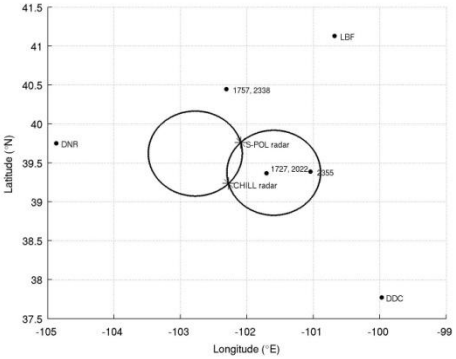

Fig. 3. Sounding and radar locations for the STEPS campaign. Numbers represent the time (UTC) of mobile soundings. Circles represent dual-Doppler lobes with a crossing angle of 30°.

The CHILL and S-pol data fields were interpolated to a Cartesian grid with spacing of 1.0 km in the horizontal and 0.5 km in the vertical (up to 20 km AGL) using NCAR's Sorted Position Radar INTerpolator (SPRINT: Mohr and Vaughn 1979; Miller et al. 1986) software. Once again, the dual-Doppler processing was done using the CEDRIC software. The final dual-Doppler files were obtained from Timothy Lang (CSU) and contained vertical velocity values computed using a downward integration technique in CEDRIC. A complete explanation of the radar quality control measures taken and dual-Doppler analysis technique can be found in Tessendorf et al. (2005).

The second storm studied was a supercell that went through the STEPS CHILL and S-pol dual-Doppler domain between 2130 UTC 29 June 2000 and 0115 UTC 30 June 2000. The supercell formed just ahead of a dryline with an approaching mesoscale cold front to the north (Kuhlman et al. 2006). The storm's first radar echo appeared around 2130 UTC near the borders of Colorado, Nebraska, and Kansas. The strongest portion of the storm was around 2338 UTC which is shown in Fig. 4. The storm lasted for almost four hours, moving southeastward, before being overtaken by an MCS in central Kansas.

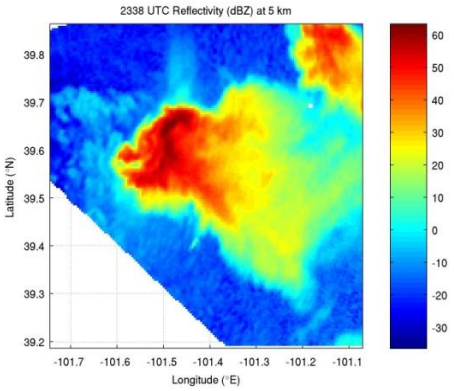

Fig. 4. Horizontal cross section of the STEPS supercell at a height of 5 km (2338 UTC).

3. METHODOLOGY

The first step in the level of neutral buoyancy comparison was to choose a sounding for each storm that best represented the pre-storm environment. Next, CAPE calculations (SBCAPE and MLCAPE) from all available soundings were examined to demonstrate the variability in parcel theory itself. These calculations stress the importance of choosing an air parcel that most accurately portrays the convective environment being studied.

For both cases, horizontal cross sections of vertical velocity were plotted to determine which part of each storm would undergo analysis. A box was simply drawn around the area where the greatest vertical velocity values were present. One large box was drawn rather than several smaller boxes for simplicity. This was done for horizontal cross sections every 1 km in height, beginning at 1 km and ending at 16 km for each radar scan. Although there is more than just a single convective center in some cases, the analysis box was focused on the most significant updraft core and extended to the same amount of grid points for each height and time slice.

For the LBA squall line, cross sections of vertical velocities were analyzed to determine that a 45x34 grid point box was necessary to include the strongest updrafts throughout the height of the storm as well as its duration. Figure 5 shows an example cross section taken at an altitude of 13 km.

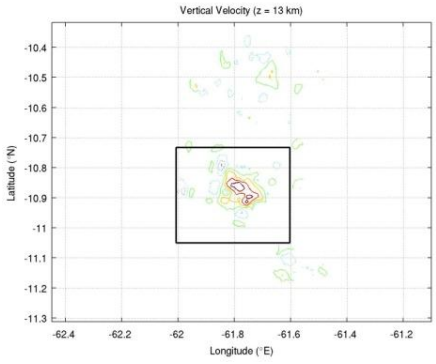

Fig. 5. Example horizontal cross section at 13 km (2050 UTC) used to determine analysis box (45x35 grid point box) for the TRMM-LBA squall line. Solid lines indicate positive vertical velocity values while dashed lines indicate negative vertical velocity values.

Horizontal cross sections of vertical velocity for the STEPS case underwent the same analysis. However, the grid box was enlarged (45x60 box) to include a much larger area of strong updrafts which is often seen in supercells as compared to squall lines and other storm types. An example cross section at 13 km can be seen in Fig. 6.

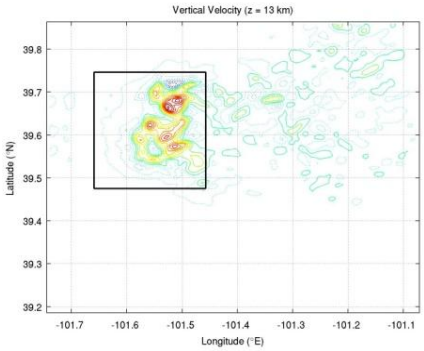

Fig. 6. Same as Fig. 5 but at 2338 UTC for the STEPS supercell (45x60 grid point box).

Lastly, the total vertical divergence (*dw/dz*) was calculated for each analysis grid box. This total divergence was calculated by first taking a first order difference along each vertical column to obtain *dw/dz*, and then integrating horizontally at each vertical level to obtain the storm-wide vertical divergence at each level. Note that maximum detrainment occurs at the level where vertical divergence is most negative, i.e. at the altitude of maximum vertical convergence and maximum horizontal divergence.

4. RESULTS

4.1 *Parcel Theory LNB*

Table 1 displays the SBCAPE, MLCAPE, and the corresponding LNB values for the TRMM-LBA squall line estimated from environmental soundings. As can be seen in Table 1, a great extent of variability is shown between calculations at different sounding stations. Although each station being at different distances from the leading edge of the squall line makes a difference in the CAPE and LNB calculations, not all variability can be attributed to this factor. Also shown in Table 1, not all upper air measurements were taken at every station at every time interval. However, the temporal and spatial resolution is significantly greater than at regular weather stations, where there are only a few soundings per day and large regions have no sounding stations at all. Therefore, the variability seen here is an even more significant factor, with the likelihood of a representative sounding being very low. Table 2 displays the SBCAPE, MLCAPE, and the corresponding LNB values

	Abracos Hill				Rebio Jaru				Rolim de Moura			
Time	**SBCAPE**	**LNB**	**MLCAPE**	**LNB**	**SBCAPE**	**LNB**	**MLCAPE**	**LNB**	**SBCAPE**	**LNB**	**MLCAPE**	**LNB**
0600 UTC					291	8.3	1827	9.6	1136	13.7	1182	13.1
0900 UTC					3	5.0	167	6.9				
1200 UTC	1363	13.8	1526	14.0	176	6.9	1046	11.7	1716	14.8	963	11.4
1500 UTC					4918	16.2	2150	14.7				
1800 UTC	2114	15.3	901	13.4	3170	15.7	4855	14.9	9459	17.1	5285	15.3
2100 UTC					5692	15.8	6202	15.3	9398	17.1	6266	15.7

Table 1. CAPE and LNB values estimated from environmental soundings taken during the TRMM-LBA campaign on 26 January 1999. The first two columns of each station display the calculated surface-based CAPE (J kg^{-1}) and LNB (km) values. The last two columns of each station display the calculated mixed-layer CAPE (J kg^{-1}) and LNB (km) values. The MLCAPE was calculated with a 1000-m mixed layer parcel.

Time	SBCAPE	LNB	MLCAPE	LNB
1727 UTC	1384	11.7	2575	12.3
1757 UTC	2881	13.0	2694	12.2
2022 UTC	2265	12.5	5803	13.7
2338 UTC	1841	12.6	2303	12.2
2355 UTC	1707	10.9	315	8.7

Table 2. CAPE and LNB values estimated from environmental soundings taken during the STEPS campaign on 29 June 2000. The first two columns are the surface-based CAPE (J kg^{-1}) and LNB (km) values for each mobile sounding. The last two columns are the mixed-layer CAPE (J kg^{-1}) and LNB (km) values. The MLCAPE was calculated with a 1000-m mixed layer parcel.

for the STEPS supercell. As in Table 1, Table 2 also displays a great extent of variability between calculations at different mobile sounding times.

4.2 *Observed LNB*

The total vertical divergence profile for the most active times of the squall line (1950-2030 UTC) can be seen in Fig. 7. At 2000 UTC, the level of maximum detrainment is between 12 and 13 km. At 2010 UTC, this level has dropped slightly to around 11 km. As the storm continues to move through the dual-Doppler lobes and more of a stratiform region is being sampled, the level of maximum detrainment continues to drop dramatically.

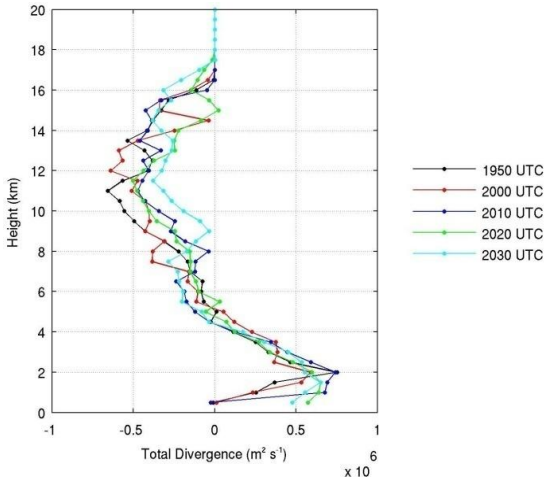

Fig. 7. Total vertical divergence profile (*dw/dz*) for the TRMM-LBA squall line for the most active parts of the squall line (1950-2030 UTC).

Figure 8 displays the time averaged total vertical divergence profile for the TRMM-LBA squall line for all analysis times available (1950-2210 UTC) indicating that the level of maximum detrainment is between 10.5 and 11 km. A large difference can be seen when comparing the observed LNB in this case to the calculated LNB values seen in Table 1. This observation strongly demonstrates the uncertainty in using environmental soundings for LNB calculations.

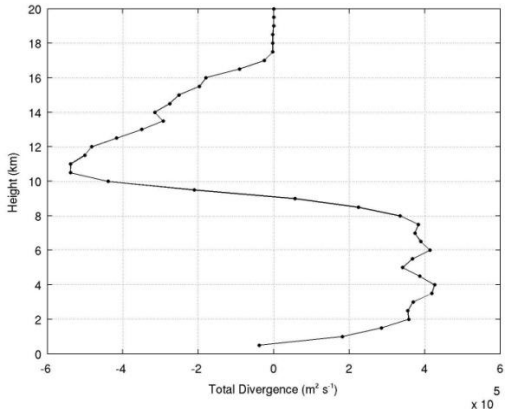

Fig. 8. Time averaged total vertical divergence profile (*dw/dz*) for the TRMM-LBA squall line.

The total vertical divergence profile for the STEPS supercell is shown in Fig. 9. With many more analysis times than the LBA case, changes in the level of maximum detrainment can be seen more easily as the storm evolves. The earlier times indicate a slightly lower level of maximum detrainment (around 12 km) than the later times (around 14 km). This makes sense due to the fact that the storm was still intensifying during the earlier times and reached a more mature stage between 0023 and 0030 UTC.

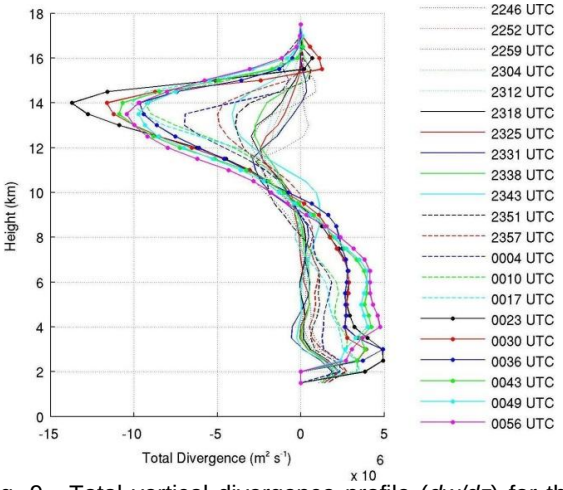

Fig. 9. Total vertical divergence profile (*dw/dz*) for the STEPS supercell.

Figure 10 displays the time averaged total vertical divergence profile for the STEPS supercell. Once again, a large difference can be seen when comparing the observed LNB around 13.5 km to the parcel theory estimated LNB values seen in Table 2.

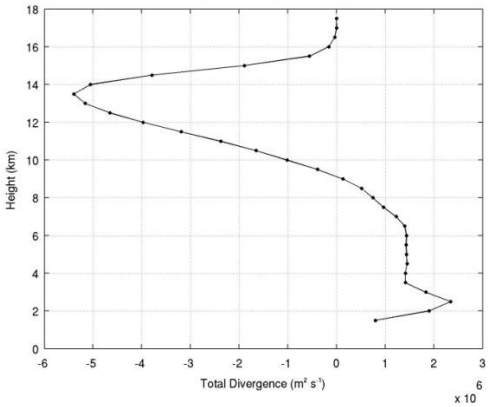

Fig. 10. Same as Fig. 8 but for the STEPS supercell.

5. SUMMARY AND CONCLUSIONS

This research confirms that the traditional method of using parcel theory and environmental soundings to estimate the LNB in convective storms is insufficient A

new methodology is presented to more accurately define where mass is most likely being deposited utilizing dual-Doppler radar data. By calculating the total divergence from the vertical velocity field, the level of maximum detrainment is able to be determined.

The importance of the LNB has been neglected in many atmospheric research endeavors. However, researchers must keep in mind that being able to correctly determine where maximum detrainment is taking place in deep convection plays a critical role in the amount of mass being deposited by a storm. By more accurately estimating this level of maximum detrainment, transport models will in turn be able to more accurately simulate the upper troposphere and lower stratosphere.

6. FUTURE WORK

Future work includes completing the analysis of the two cases presented in this study. Time-integrated results will be determined to create a clear picture of where and how much mass is being deposited by the aforementioned storms. Also, the total divergence profiles will be calculated for only upward velocities which should prove useful in more accurately determining maximum detrainment heights. Finally, the incorporation of density into the total divergence calculations will also be investigated.

The TRMM-LBA and STEPS cases used in this study allowed both a squall line and a supercell to be studied. Future work will incorporate a multicell storm which occurred in eastern North Dakota and western Minnesota on 5 June 2006. Dual-Doppler processing will be done using the University of North Dakota C-band radar and the NWS WSR-88D radar located near Mayville, ND (KMVX).

Lastly, current work has incorporated the use of radio occultation (RO) data as a means of collecting atmospheric soundings. Statistics have been completed comparing RO soundings with NWS upper air measurements across the Northern Plains. Differences in water vapor between the two datasets are being investigated and how these differences may affect CAPE and LNB estimations.

ACKNOWLEDGMENTS

This research was funded by ND EPSCoR New Faculty Startup project number 43700-2210-UND0013942 and NSF grant number EPS-0814442. Special thanks to Timothy Lang (CSU) for the processed dual-Doppler radar files from the STEPS field campaign.

REFERENCES

Alexander, M. J., P. T. May and J. H. Beres, 2004: Gravity waves generated by convection in the Darwin area during the Darwin Area Wave Experiment. *J. Geophys. Res.*, **109** (D20S04), doi:10.1029/2004JD004729.

Cifelli, R., W. A. Petersen, L. D. Carey, S. A. Rutledge, and A. F. da Silva Dias, Maria, 2002: Radar observations of the kinematic, microphysical, and precipitation characteristics of two MCSs in TRMM-LBA. *J. Geophys. Res.*, **107** (D20), doi:10.1029/2000JD000264.

Cohen, C., 2000: A quantitative investigation of entrainment and detrainment in numerically simulated cumulonimbus clouds. *J. Atmos. Sci.*, **57**(10), 1657-1674.

Dickerson, R. R., 1987: Thunderstorms: An important mechanism in the transport of air pollutants. *Science*, **235**, 460-465.

Doswell, C. A., III, and P. M. Markowski, 2004: Is buoyancy a relative quantity? *Mon. Wea. Rev.*, **132**, 853-863.

Emanuel, K. A., 1991: A scheme for representing cumulus convection in large-scale models. *J. Atmos. Sci.*, **48**(21), 2313-2335.

Kain, J. S. and J. M. Fritsch, 1990: A one-dimensional entraining/detraining plume model and its application in convective parameterization. *J. Atmos. Sci.*, **47**(23), 2784-2802.

Kuhlman, K. M., C. L. Ziegler, E. R. Mansell, D. R. MacGorman, and J. M. Straka, 2006: Numerically simulated electrification and lightning of the 29 June 2000 STEPS supercell storm. *Mon. Wea. Rev.*, **134**, 2734-2757.

Kummerow, C., W. S. Olson, and L. Giglio, 1996: A simplified scheme for obtaining precipitation and vertical hydrometeor profiles from passive microwave sensors. *IEEE Trans. Geosci. Remote Sens.*, **34**, 1213-1232.

Lang, T. J., and S. A. Rutledge, 2002: Relationships between convective storm kinematics, precipitation, and lightning. *Mon. Wea. Rev.*, **130**, 2492-2506.

Mapes, B., and R. A. Houze Jr., 1995: Diabatic divergence profiles in western Pacific mesoscale convective systems. *J. Atmos. Sci.*, **52**, 1807-1828.

Mohr, C. G., and L. J. Miller, 1983: CEDRIC - A software package for cartesian space editing, synthesis, and display of radar fields under interactive control. *Preprints, 21st Conf. on Radar Meteorology*, Boston, MA, Amer. Meteor. Soc., 559-574.

Mohr, C. G., and R. L. Vaughn, 1979: An economical approach for Cartesian interpolation and display of reflectivity factor data in three-dimensional space. *J. Appl. Meteor.*, **18**, 661-670.

Mohr, C. G., L. J. Miller, R. L. Vaughan, and H. W. Frank, 1986: The merger of mesoscale data sets into a common cartesian format for efficient and systematic analyses. *J. Atmos. Oceanic Technol.*, **3**, 143-161.

Miller, L. J., C. G. Mohr, and A. J. Weinheimer, 1986: The simple rectification to Cartesian space of folded radial velocities from Doppler radar sampling. *J. Atmos. Oceanic. Technol.,* **3**, 162-174.

Mullendore, G. L., D. R. Durran, and J. R. Holton, 2005: Cross-tropopause tracer transport in midlatitude convection. *J. Geophys. Res.*, **110** (D06113), doi:10.1029/2004JD005059.

Olson, W. S., C. D. Kummerow, Y. Hong, and W. K. Tao, 1999: Atmospheric latent heating distributions in the tropics derived from satellite passive microwave radiometer measurements. *J. Appl. Meteorol.*, **38**, 633-664.

Schumacher, C., R. A. Houze, Jr, and I. Kraucunas, 2004: The tropical dynamical response to latent heating estimates derived from the TRMM precipitation radar. *J. Atmos. Sci.*, **61**, 1341-1358.

Stenchikov, G., and Coauthors, 1996: Stratosphere-troposphere exchange in a midlatitude mesoscale convective complex 2. Numerical simulations. *J. Geophys. Res.*, **101**, 6837-6851.

Tao, W. K., J. Simpson, C. H. Sui, B. Ferrier, S. Lang, J. Scala, M. D. Chou, and K. Pickering, 1993: Heating, moisture, and water budgets of tropical and middle latitude squall lines: comparisons and sensitivity to longwave radiation. *J. Atmos. Sci.*, **50**, 673-690.

Tessendorf, S. A., L. J. Miller, K. C. Wiens, and S. A. Rutledge, 2005: The 29 June 2000 supercell observed during STEPS. Part 1: kinematics and microphysics. *J. Atmos. Sci.*, **62**, 4127-4150.

Yang S., and E. A. Smith, 1999: Four-dimensional structure of monthly latent heating from SSM/I satellite measurements. *J. Clim.*, **12**, 1016-1037.